EFFECT OF THE POROUS SKELETAL IRON STRUCTURE ON THE INFILTRATION OF ALUMINUM MELTS

P.I. Loboda,[1] A.V. Minitsky,[1,2] Ye.G. Byba,[1] M.O. Sysoev,[1] and S.V. Radchuk[1]

The infiltration of aluminum melts into porous metal skeletons produced by powder metallurgy methods, including 3D printing, under a pressure gradient was studied. The densification of compacts made of iron powder with various blowing additions was examined. The minimum pressures at which 35–40% porosity was reached were found to be 150–200 MPa. The use of metal iron shavings allowed a porous skeleton to be formed at a lower pressure (100 MPa). The minimum pore size (400 µm) ensuring complete filling of the porous skeleton with an aluminum melt heated to 760–780ºC under a pressure gradient was established. The potential production of iron–aluminum composites without the formation of chemical compounds was shown. A thin discrete layer 5–10 µm thick was observed at the interface between iron and aluminum, where the iron skeleton became saturated with aluminum. This layer provides better adhesion between the iron skeleton and the aluminum melt. The absence of chemical compounds in the Fe–Al system in impregnation conditions is explained by the process kinetics: the components cannot react with each other within several seconds. The effect exerted by the type of porous skeletal structure on the compressive strain of the iron–aluminum composites was established. The greatest compression strength (~400 MPa) was shown by the samples produced from 3D skeletons. The stress–strain curves for the samples with 3D skeletons show two bends: one is in the range 60–70 MPa (beginning of plastic deformation) where strain hardening occurs and strain increases to 20–22% and the other begins at 230–240 MPa and determines the bulk deformation of the samples. The highest yield stress was observed for the samples with shavings-based skeletons (115.2 MPa), which is associated with a high contact surface area of the shaving particles that are randomly intertwined. Accordingly, the lowest characteristics were shown by the samples with skeletons consisting of powder particles with the minimum contact area.

Keywords: infiltration, porous skeleton, powder, shavings, 3D printing, iron, aluminum, pores, strain.

INTRODUCTION

The development of modern aviation and mechanical engineering calls for materials with predetermined characteristics. The infiltration of melts into porous skeletons is an effective way of producing composites with high physical and mechanical properties and allows the composition, structure, and shape of finished articles to be

[1]National Technical University 'Igor Sikorsky Kyiv Polytechnic Institute', Kyiv, Ukraine.

[2]To whom correspondence should be addressed; e-mail: minitsky@i.ua.

controlled. The papers dealing with the infiltration of aluminum melts into porous skeletons focus on ceramic matrices made of aluminum oxide and silicon carbide [1–4]. As far as the impregnation of metallic skeletons is concerned, there are papers on the infiltration of aluminum melts into porous nickel and titanium. Porous titanium is effectively used to develop composites for medical applications [5–7].

The infiltration of molten copper, silver, magnesium, and other fusible metals into sintered porous iron skeletons has been adequately studied to date [8, 9]. Experiments on the infiltration of aluminum melts into iron skeletons have restrictions because iron is poorly wetted by aluminum [10]. There was an attempt to infiltrate aluminum into an iron skeleton by immersing it into a liquid aluminum melt [11]. However, iron and aluminum actively interacted to form intermetallic phases (in particular, $FeAl_3$). As a result, the pores closed and infiltration stopped. To overcome this obstacle, an iron skeleton was impregnated with aluminum at a pressure of 10 MPa in an autoclave chamber when compressed argon was fed into it. The aluminum melt filled the pores, but a significant number of intermetallic phases formed in the material and increased its hardness and brittleness. Moreover, the composite had a residual porosity of 15–18%, also affecting its properties. Hence, the development of iron-matrix skeletal composites is of both scientific and applied interest since these materials combine excellent mechanical and thermal properties [12–14].

Our objective is to examine how a porous iron skeleton produced by different methods is impregnated with an aluminum melt and determine how the type of porous skeletal structure influences the compressive strain of the composites.

EXPERIMENTAL PROCEDURE

Powder metallurgy methods, including additive 3D printing processes, were used to produce porous skeletons.

We employed static pressing to produce a skeletal structure from an atomized iron powder with an average particle size of 350–400 μm (Fig. 1). The compacts with a height-to-diameter ratio of ~1.5 were pressed at 150–300 MPa. To increase the total porosity of the samples by 5–7%, blowing agents, such as ammonium carbonate and carbamide, were added at the same pressure to the iron powder. The effect of a blowing agent on porosity of the samples was studied. At a pressure of 150–200 MPa, the total porosity was 35–40% and the highest porosity (~40%) was reached with carbamide as a blowing agent (Fig. 2). The minimum pressure at which the iron powder of this size fraction can be molded is 150 MPa.

We prepared pellets from iron shavings (metal scrap). This approach can be promising in terms of metal scrap recycling. The shaving particles are flaky and are compacted at low pressures (100–150 MPa); thus, the compacts acquire 35–40% porosity without a blowing agent. The pellets were sintered at 1100ºC for 1 h in a hydrogen atmosphere.

We applied 3D printing with selective laser melting employing a Realized SLM50 printer to make porous skeletons. In iron powder of the–63+45 μm size fraction was used to create a single layer up to 70 μm. The laser power was 75 W and the scanning rate was 0.4 m/sec, corresponding to the 20 μm distance between the processing points and the 50 μsec exposure time at one point.
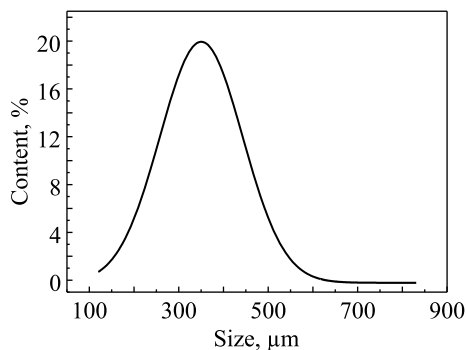
Fig. 1. Grain-size composition of the iron powders
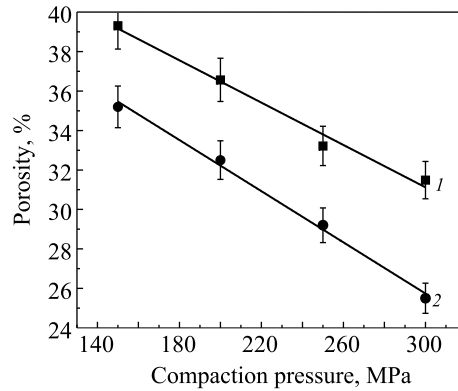
Fig. 2. Porosity of the samples with different blowing agents versus compaction pressure: *1*) carbamide, *2*) ammonium carbonate

Figure 3 shows the structures of porous iron skeletons produced by different methods. According to metallographic analysis, the pore size is 50–100 μm for the powder samples and 400–450 μm for the 3D-printed samples. The samples of both types have almost the same size and shape of pores, being uniformly distributed over the volume. The samples prepared from iron powder shavings have branched pore channels of different shape and size, resulting from the flaky structure of shaving particles and plastic deformation processes that occur in static pressing.

The next step was to infiltrate the AK7 aluminum melt into the porous iron skeletons. A dedicated workbench was used for this purpose to create a pressure gradient.
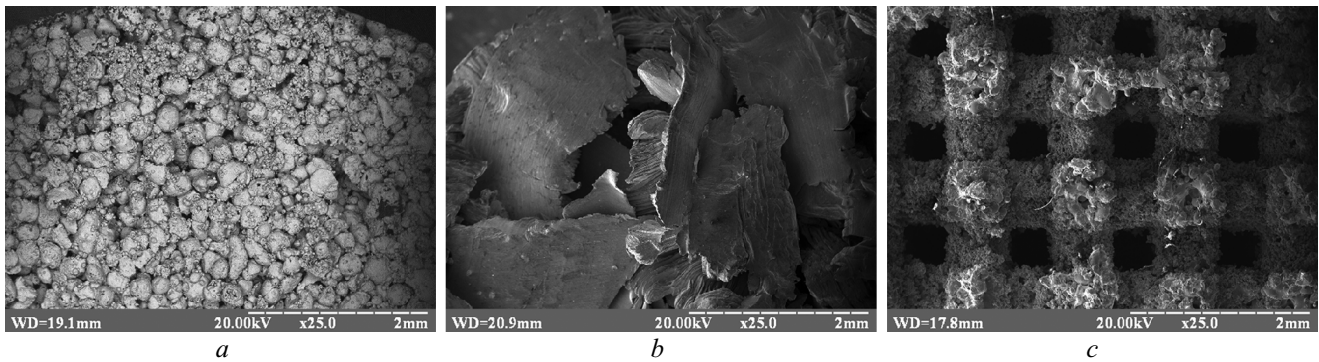
Fig. 3. Structures of porous skeletal materials produced from iron powder (*a*), iron shavings (*b*), and 3D skeletons (*c*)
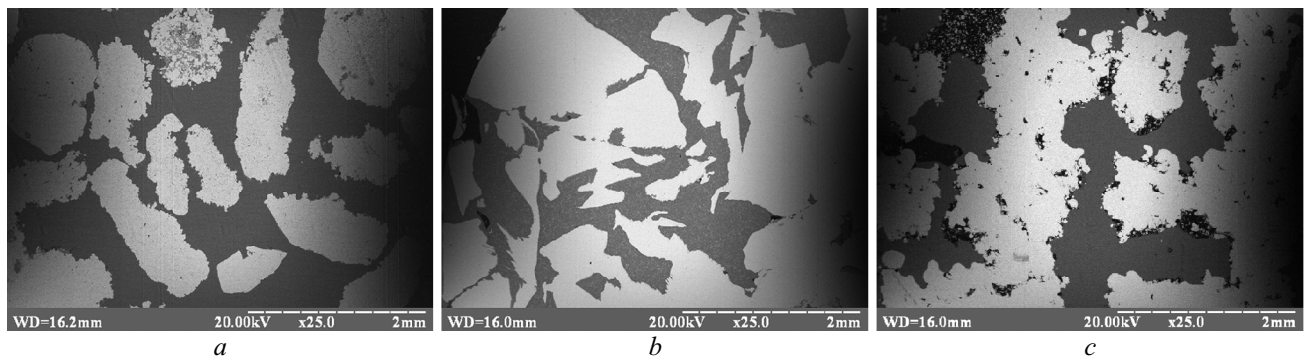
Fig. 4. Microstructures of the samples produced from iron powder (*a*), iron shavings (*b*), and 3D skeletons (*c*) impregnated with the AK7 aluminum melt

653
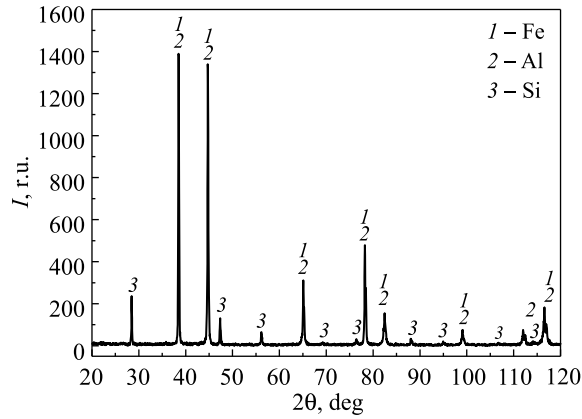
Fig. 5. X-ray diffraction pattern for the samples with porous iron skeletons impregnated with the AK7 aluminum melt

A porous skeleton was placed into a special steel mold into which aluminum molten at 760–780°C was poured. Then a vacuum booster pump was switched on to impregnate the skeleton at 2–4 kPa for 3–5 sec.

The cylindrical composite samples with a height-to-diameter ratio of 1.5 were tested by compression employing calibrated Ceramtest and Tiratest 28100 universal machines.

DISCUSSION OF RESULTS

The microstructural images (Fig. 4) show that aluminum is distributed over the volume of the porous iron skeleton, filling open pores. The minimum pore size that promotes the infiltration of aluminum melts under a pressure gradient is 400 μm.

The composites (Fig. 5) contain phases such as α-Fe, Al, and Si solid solutions; i.e., the material has no intermetallic phases that commonly form in the Fe–Al system. X-ray spectrometry confirmed that were no intermetallics in the system. Note that a thin discrete layer 5–10 μm thick was observed at the interface between iron and aluminum, in which the iron skeleton impregnated with aluminum (Fig. 6). Such interaction at the metal interface should promote better adhesion between the matrix and skeleton.
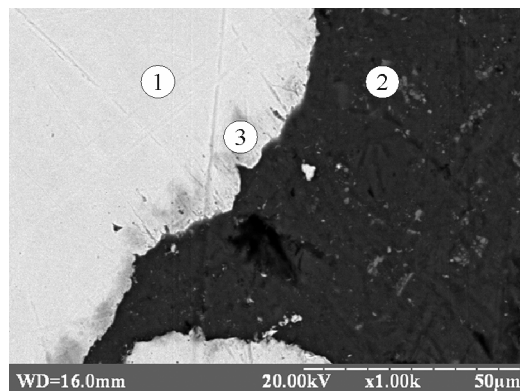
Chemical composition of the Fe–Al material

Element	Point		
	1	2	3
Fe	99.87	0.63	96.48
Al	–	82.45	3.52
Si	–	16.92	–

Fig. 6. X-ray spectroscopy of the material with an iron skeleton impregnated with the AK7 aluminum melt
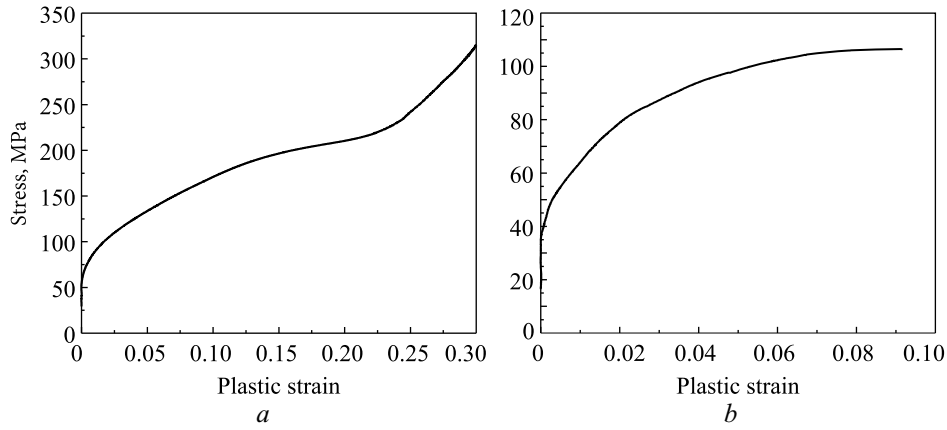
Fig. 7. Stress–strain curves for compression of the composites produced from 3D skeletons (*a*) and iron powder (*b*)

TABLE 1. Mechanical Properties of the Materials in Compression

Type of skeleton	Yield stress σ_{02}, MPa	Compression strength σ_c, MPa	Strain ε, %
Powder	46.8	106.5	9.2
Shavings	115.2	160.8	7.8
3D	68.1	400.1	31.8

There are no intermetallic phases in the composite because vacuum infiltration lasts within several seconds and the components have no time to react with each other. Accordingly, the mechanical properties of such skeletal materials should be greater than those of the materials infiltrated by immersion into the melt with long-term holding.

Mechanical tests showed that the highest compressive strength (~400 MPa) was exhibited by the samples with 3D skeletons (Table 1). The highest yield stress was observed for the samples with shavings-based skeletons (115.2 MPa). This is associated with a great contact surface area of the shaving particles being randomly intertwined. Hence, the lowest characteristics are exhibited by the samples with a skeleton consisting of powder particles having the minimum contact area. There are also individual areas where no skeleton formed.

Analyzing the fracture behavior of the skeletal composites in compression, we noted the difference in deformation of the samples produced from 3D skeletons and those produced by powder compaction (Fig. 7). Thus, plastic deformation of the powder skeleton begins already at 50 MPa and is followed by its failure at ≈100 MPa. There are two bands on the stress–strain curves for the samples with 3D skeletons: one bend is observed at 60–70 MPa (beginning of plastic deformation) when strain hardening occurs and strain increases to 20–22% and the other bend starts at 230–240 MPa and determines bulk deformation of the samples (change in geometrical parameters).

Note also that a part of the impregnated samples with 3D skeletons did not fail at all under compression. Their strain was higher than 30%; i.e., the composites have high ductility.

CONCLUSIONS

The infiltration of an aluminum melt into porous iron skeletons produced by powder metallurgy methods, including 3D printing, under a pressure gradient has been studied. The minimum pore size that promotes the infiltration of the aluminum melt has been found to be 400 μm.

Skeletal Fe–Al composites can be produced without the formation of intermetallic phases. Two-step deformation has been established for 3D skeletons with a compressive strength of ~400 MPa.

The results can be used to develop heterogeneous materials with high strength and electrical and thermal conductivity.

REFERENCES

1. T.E. Wilkes, M.L. Young, R.E. Sepulveda, D.C. Dunand, and K.T. Faber, "Composites by aluminum infiltration of porous silicon carbide derived from wood precursors," *Scr. Mater.*, **55**, 1083–1086 (2006).

2. Kalkanli Ali, Durmaz Tayfun, Kalemtas Ause, and Arslan Gursoy, "Melt infiltration casting of alumina silicon carbide and boron carbide reinforced aluminum matrix composites," *J. Mater. Sci. Eng.*, **6**, No. 4, 1–5 (2017), DOI: 10.4172/2169-0022.1000357.

3. A. Boczkowska, P. Chabera, A.J. Dolata, M. Dyzia, and A. Ozieblo, "Porous ceramic—metal composites obtained by infiltration methods," *Metalurgia*, **52**, No. 3, 345–348 (2013).

4. B. Lipowska, B. Psiuk, M. Cholewa, and L. Kozakiewich, "Preliminary test of cellular SiC/Iron alloy composite produced by a pressureless infiltration technique," *Arch. Foundry Eng.*, **17**, No. 1, 115–120 (2017).

5. Y.B. Choi, K. Matsugi, and G. Sasaki, "Development of intermetallic compounds reinforced Al alloy composites using reaction of porous nickel and aluminum," *Mater. Trans.*, **54**, No. 4, 595–598 (2013).

6. L.A. Dobrzanski, A.D. Dobrzanska-Danikiewicz, T.G. Gawel, and A. Achtelic-Franczak, "Selective laser sintering and melting of pristine titanium and titanium Ti6Al4V alloy powders and selection of chemical environment for etching of such materials," *Arch. Metall. Mater.*, **60**, 2039–2045 (2015).

7. L. Dobrzanski, G. Matula, A.D. Dobrzanska-Danikiewicz, P. Malara, and M. Kremzer, "Composite materials infiltrated by aluminum alloys based on porous skeleton from alumina, mullite and titanium produced by powder metallurgy techniques," in: *Powder Metallurgy—Fundamentals Case Studies* (2017), pp. 95–137, DOI: 10.5772/65377.

8. V.A. Dovydenkov, E.V. Solovieva, O.S. Zvereva, and N.A. Kuzina, "Infiltration of brass into heterogeneous porous iron ingots," *Vest. Tekhnol. Univ.*, **19**, No. 13, 67–70 (2016).

9. D.M. Karpinos, *Composite Materials: Handbook* [in Russian], Naukova Dumka, Kyiv (1985), p. 594.

10. Esa Vuorinen and Magnus Odén, "Limitation of the infiltration in brazing of porous P/M parts," in: *Controlling Infiltration when Brazing P/M Parts and during Manufacture of Aluminum Metal Matrix Composites*, Department of Applied Physics and Mechanical Engineering Division of Engineering Materials Lulea University of Technology SE-97187, Lulea, Sweden (2004), pp. 23–31.

11. L.I. Tuchinskii, *Composite Materials Produced by Impregnation* [in Russian], Metallurgiya, Moscow (1986), p. 208.

12. Alexander E. Pawlowski, Zachary C. Cordero, Matthew R. French, Thomas R. Muth, J. Keith Carver, Ralph B. Dinwiddie, Amelia M. Elliot, Amit Shyam, and Derek A. Splitter, "Damage-tolerant metallic composites via melt infiltration of additively manufactured preforms," *Mater. Des.*, **127**, 346–351 (2017).

13. Moona Girija, R.S. Walia, Rastogi Vikas, and Sharma Rina, "Aluminum metal matrix composites: A retrospective investigation," *Indian J. Pure Appl. Phys.*, **56**, 164–175 (2018).

14. M.O. Bodunrin, K.K. Alaneme, and L.H. Chown, "Aluminum matrix hybrid composites: a review of reinforcement philosophies; mechanical, corrosion and tribological characteristics," *J. Mater. Technol.*, **4**, No. 4, 434–445 (2015).